ISSN 1063-7761, Journal of Experimental and Theoretical Physics, 2023, Vol. 137, No. 4, pp. 486–491. © Pleiades Publishing, Ltd., 2023.
Russian Text © The Author(s), 2023, published in Zhurnal Eksperimental'noi i Teoreticheskoi Fiziki, 2023, Vol. 164, No. 4, pp. 563–568.

Optical Linear Dichroism in the *ab*-Plane of $NdFe_3(BO_3)_4$ Ferroborate

K. N. Boldyrev[a], M. Diab[b], I. A. Gudim[c], and M. N. Popova[a,*]

[a] *Institute of Spectroscopy, Russian Academy of Sciences, Troitsk, Moscow, 108840 Russia*
[b] *Moscow Institute of Physics and Technology (State University), Dolgoprudnyi, Moscow oblast, 141700 Russia*
[c] *Kirenskii Institute of Physics, Siberian Branch, Russian Academy of Sciences, Krasnoyarsk, 660036 Russia*
**e-mail: popova@isan.troitsk.ru*

Received April 27, 2023; revised May 20, 2023; accepted May 25, 2023

Abstract—The high-resolution optical absorption spectra of $NdFe_3(BO_3)_4$ single crystals have been recorded at temperatures from 4 to 40 K in the IR range of *f*–*f* transitions in a Nd^{3+} ion. Light linearly polarized at different angles to the C_2 axes in the basal plane has been passed along the trigonal C_3 axis. Below the temperature of magnetic moment ordering into a collinear antiferromagnetic structure ($T_N \approx 30$ K), dichroism, that is, the absorption versus polarization dependence, arises. The temperature and angular dependences of dichroism indicate that the magnetic moments of iron are directed along the C_2 axes up to about 17 K, the number of domains with variously directed C_2 axes being different. The mechanism of linear dichroism has been discussed. Below 17 K, a smooth transition to the helicoidal magnetic phase has been observed, with the collinear phase coexisting with the helicoidal one. Data presented in this article contradict the earlier concept of magnetic moments fluctuating in the low-temperature phase near the C_2 axis within the $\pm 10°$ interval.

DOI: 10.1134/S1063776123100011

1. INTRODUCTION

Neodymium ferroborate $NdFe_3(BO_3)_4$, a member of the multiferroic family with a huntite mineral structure, is notable for a high magnetically controlled electrical polarization, a giant quadratic magnetoelectric effect, and an intriguing magnetic structure [1–4]. The crystal structure of neodymium ferroborate is described by the space symmetry group *R*32 at all temperatures. Its structure is characterized by the presence of helical chains made up of iron ions, which are directed along the *c* (C_3) axis. They are interconnected by BO_3 groups and mutually isolated NdO_6 prisms (having the point symmetry group D_3) [5, 6]. At temperature $T_N \approx 30$ K [2, 7–9], the iron subsystem becomes ordered, acquires an easy-plane commensurate collinear structure, and magnetizes the rare-earth subsystem [2–4, 8]. The magnetic moments of iron and neodymium are oriented ferromagnetically in the *ab* basal plane along the *a* (C_2) axis and antiferromagnetically in between adjacent planes [3].

According to neutron diffraction data, below $T_{IC} \approx 19$ K [2] (in other sources, 13.5 [3], 15 [9], and16 K [4]) the magnetic structure gradually changes to an incommensurate antiferromagnetic helicoidal one in which magnetic moments are still confined in the basal plane. This transition is due to the magnetic frustration in between the Nd and Fe sublattices [4]. Single crystal neutron diffraction and spherical neutron polarimetry data show that (i) the helicoidal structure is not harmonic (higher harmonics are observed in scattering) and (ii) a long-period single-chirality antiferromagnetic helix arises [3].

Using X-ray resonant magnetic scattering it was shown [4] that the commensurate collinear structure disappears below T_{IC} incompletely, coexisting with the incommensurate helicoidal one. Note that in the work [10] by L.A. Prozorova and coauthors, data on the magnetization and magnetic resonance for a quasi-2D antiferromagnet on a triangular lattice $KFe(MoO_4)_2$ were explained under the assumption of coexisting collinear and helical structures. A model of magnetic structure with magnetic planes of two types, that is, helically and collinearly ordered, was suggested [10]. For quasi-1D antiferromagnet $NdFe_3(BO_3)_4$, the coexistence mechanism of helical and collinear phases was not discussed [4].

However, Mössbauer spectroscopy data taken of single-crystalline $NdFe_3(BO_3)_4$ at 295, 40, 25, and 4.2 K did not reveal the low-temperature incommensurate helicoidal phase and researchers suggested that

the fluctuating magnetic moments of iron are distributed within ±10° about the *a* axis at low temperatures [11]. Quite recently, a more detailed temperature dependence of Mössbauer spectra for $NdFe_3(BO_3)_4$ single crystals has been obtained [9]. It was found that the variation of the quadrupole shift with temperature in the low-temperature range correlates with the possible transition to the incommensurate phase at T_{IC}. It should be noted that temperature T_{IC} in no ways shows up in the temperature dependence of the $NdFe_3(BO_3)_4$ specific heat [2, 8].

Using a CuB_2O_4 tetragonal crystal as an example, it was shown [12] that the optical linear dichroism in the basal plane of a uniaxial crystal is a very sensitive tool for studying magnetic phase transitions and magnetic structures. Here, we applied this method to study $NdFe_3(BO_3)_4$ trigonal crystal. It is noteworthy that detailed investigations of high-resolution spectra taken of $NdFe_3(BO_3)_4$ crystals in the IR range of *f–f* transitions in a Nd^{3+} ion did not reveal any spectral features near the transition to the incommensurate phase [7, 13].

2. EXPERIMENTAL

$NdFe_3(BO_3)_4$ single crystals were grown from a bismuth trimolybdate-based solution-melt. The composition of the solution-melt was the following:

$$75\ \text{wt}\ \%\ (Bi_2Mo_3O_{12} + 3B_2O_3 + 0.6Nd_2O_3) + 25\ \text{wt}\ \%\ NdFe_3(BO_3)_4.$$

After the homogenization of the solution-melt, a purified crystal holder was reversibly submerged in it at 1200°C with a period of 1 min and a rotation rate of 30 rpm. The furnace temperature was decreased by 120°C, and the crystal holder with crystal seeds was extracted from the solution-melt in 2 h. Then, the growth was carried out by the batch method. In this method, as many as several seeds are fixed on the crystal holder. As a result, several crystals grow simultaneously under identical hydrodynamic and thermophysical conditions provided by stirring the solution–melt with the reversibly rotating crystal holder. Within 24 h, crystallites 0.5–2.0 mm in size grew up from the seeds on the crystal holder. They were sufficiently perfect and used to grow large crystals. The crystal holder with several seeds was submerged in the solution-melt, and reversible rotation was switched on. The temperature was smoothly lowered with a rate of 1°C/day. In eleven days, the growth was ceased, and the crystal holder was extracted from the solution-melt and cooled down to room temperature (for more details, see [14]).

Grown single crystals measuring about 5 × 4 × 3 mm^3 were of a good optical quality and had green color characteristic of ferroborates and natural faceting. The crystallites were cut into thin sheets so that their planes were normal to the triad axis C_3. The sheets were habitus-oriented, and their orientation was checked with a conoscopic image observed in a polarization microscope in between crossed polarizers. The conoscopic image was distinct, signifying a high setting accuracy of the axis. Samples were placed in a Sumitomo RP096 closed-cycle optical helium cryostat in such a way that the light propagated along the C_3 axis of the crystallite ($\mathbf{k} \parallel c$). The temperature could be varied from 3.5 to 300 K and be kept accurate to ±0.05 K. The transmission spectra of $NdFe_3(BO_3)_4$ crystals were recorded in the spectral interval 3000–10000 cm^{-1} using a Bruker IFS 125HR Fourier spectrometer. In the case of nonpolarized light, vectors $\mathbf{E}^\omega$ and $\mathbf{B}^\omega$ are normal to the *c* axis because of light wave transversality. Such a configuration is called α-polarization. To study the linear dichroism in the basal *ab*-plane of the crystal, a mid-IR computer-controlled rotating polarizer was set in front of the crystal. A complete polarization circle with a 5°-step was studied. In the obtained spectra, a pair of signals with a maximal difference was found and angles at which this difference was observed were fixed. Then, the detailed temperature dependences of the spectra taken at these two angles were investigated.

3. RESULTS

Figure 1a shows the low-temperature transmission spectrum of light propagating along the *c* (C_3) axis in the $NdFe_3(BO_3)_4$ crystal. The spectrum was taken in the range of IR transitions ${}^4I_{9/2} \rightarrow {}^4I_{13/2}$ and ${}^4I_{9/2} \rightarrow {}^4I_{15/2}$ in a Nd^{3+} ion. Low-frequency lines in each of the transitions are narrow, whereas high-frequency ones are broader because of phonon relaxation to lower lying levels. It should be noted that electron dipole transitions dominate in this range [13].

Figure 1b demonstrates the ratio of transmission spectra taken at 15 K when the polarizer was set along and normally to the C_2 axis in the basal *ab*-plane. A noticeable linear dichroism is seen. For the given two orientations of the polarizer, the difference between the spectra was maximal.

Figure 2 shows the low-frequency range of the ${}^4I_{9/2} \rightarrow {}^4I_{15/2}$ transition in more detail. The difference in the absorption spectra for two polarizations ($\mathbf{E}^\omega \parallel \mathbf{a}$ and $\mathbf{E}^\omega \perp a$) in the basal plane at 18 K is obvious (Fig. 2a). In Fig. 2b, this difference (the linear dichroism spectrum) is shown in the temperature interval from 33 to 4 K. At 33 K > T_N, the dichroism is absent. When the temperature becomes lower than T_N, the dichroism first smoothly grows (to about 17 K) and then drops down to 4 K. This is distinctly seen in an intensity map depicted in Fig. 3.

The integral absolute value of the dichroism versus temperature is depicted in Fig. 4. The adopted interval of integration, 5875–5890 cm^{-1} (see Fig. 2a), discards lines "freezing out" with decreasing temperature,

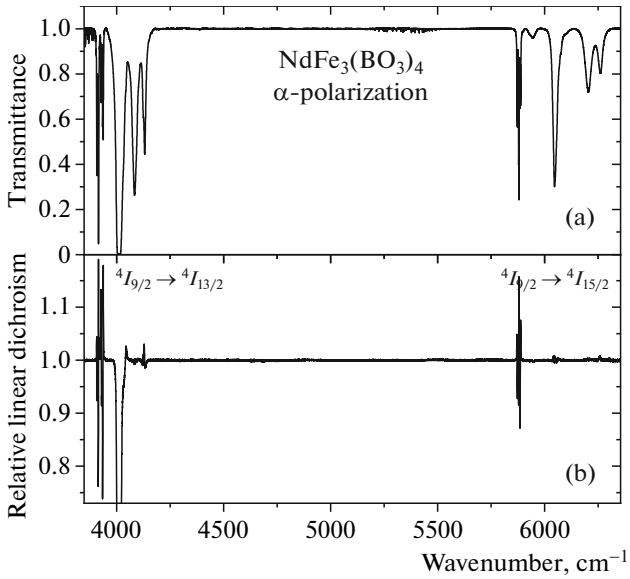

Fig. 1. (a) Transmission spectrum of $NdFe_3(BO_3)_4$ crystal in the range of ${}^4I_{9/2} \rightarrow {}^4I_{13/2}$ and ${}^4I_{9/2} \rightarrow {}^4I_{15/2}$ transitions in a Nd^{3+} ion ($T = 15$ K, α-polarization) and (b) transmission spectrum ratio for polarizations $\mathbf{E}^{\omega} \parallel a$ and $\mathbf{E}^{\omega} \perp a$ ($\mathbf{k} \parallel c$).

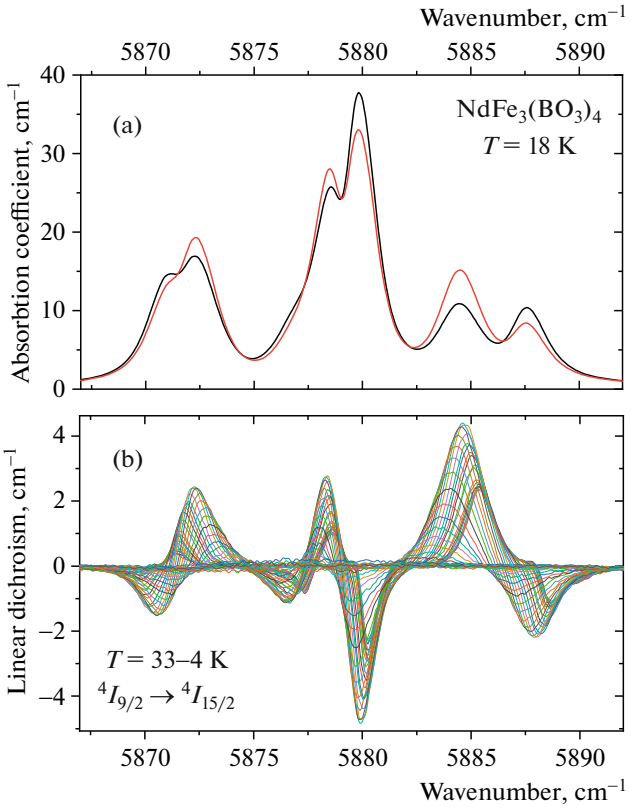

Fig. 2. (a) Absorption spectrum of $NdFe_3(BO_3)_4$ crystal at 18 K, $\mathbf{k} \parallel c$, for polarizations $\mathbf{E}^{\omega} \parallel a$ (black line) and $\mathbf{E}^{\omega} \perp a$ (red line) and (b) linear dichroism spectrum $k(\mathbf{E}^{\omega} \parallel a - \mathbf{E}^{\omega} \perp a)$ at temperatures from 33 to 4 K in the low-frequency range of the transition ${}^4I_{9/2} \rightarrow {}^4I_{15/2}$.

which are associated with transitions from the upper component of the split ground Kramers doublet.

4. DISCUSSION

In the given temperature range, the optical spectrum of $NdFe_3(BO_3)_4$ crystal is formed by transitions between Kramers doublets of a Nd^{3+} ion, which has an odd number of electrons and occupies a single position in the structure (three-fold $3a$ position with D_3 symmetry [2]). The optical transition probability in the paramagnetic phase may differ for light polarized along the c axis and light polarized normally to it [13], but it does not depend on the polarization direction in the basal ab-plane. Indeed, at $T > T_N$, the dichroism is absent. This indicates that the plane of the sample is exactly normal to the triad c (C_3) axis.

Below temperature T_N, the magnetic moments of iron orient along the C_2 axes [3]. An exchange field acting on Nd ions from the ordered magnetic subsystem of iron splits the Kramers doublets of the Nd^{3+} ion, causing splitting of spectral lines. It is easy to check that the probability of transitions between the components of split Kramers doublets will be pairwise identical: $W_+^+ = W_-^- \equiv W_1$ and $W_-^+ = W_+^- \equiv W_2$. Here, $W_1 > W_2$ if $\mathbf{E}^{\omega} \parallel a$ and vice versa if $\mathbf{E}^{\omega} \perp a$. Figure 5a depicts the diagrams of splitting and optical transitions, whereas Fig. 5b illustrates experimental spectra. Thus, when subtracting spectra relating to one line in the paramagnetic state, the contribution of two com-

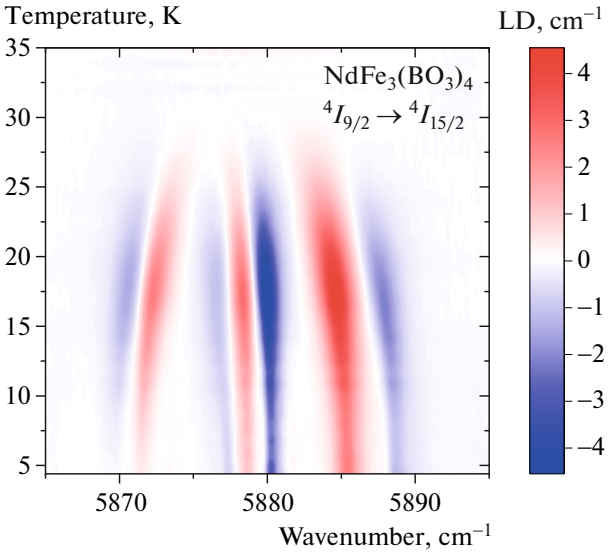

Fig. 3. Map of the optical linear dichroism (LD) $k(\mathbf{E}^{\omega} \parallel a) - k(\mathbf{E}^{\omega} \perp a)$ in the basal plane of $NdFe_3(BO_3)_4$ crystal.

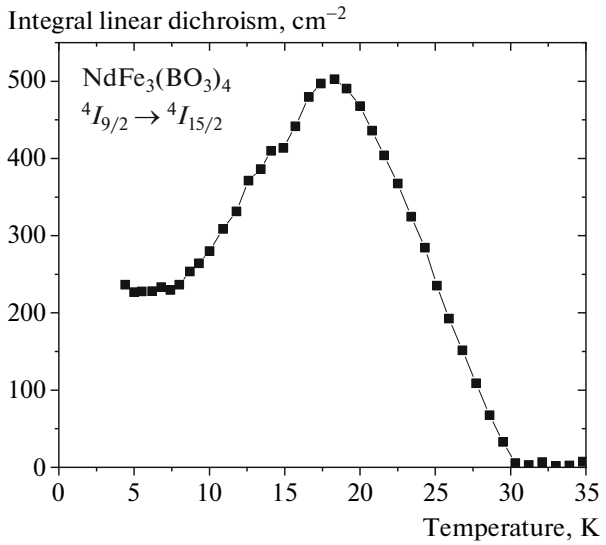

Fig. 4. Integral linear dichroism $\int |k(\mathbf{E}^\omega \parallel a) - k(\mathbf{E}^\omega \perp a)| d\nu$ in the basal plane of $NdFe_3(BO_3)_4$ crystal vs. temperature.

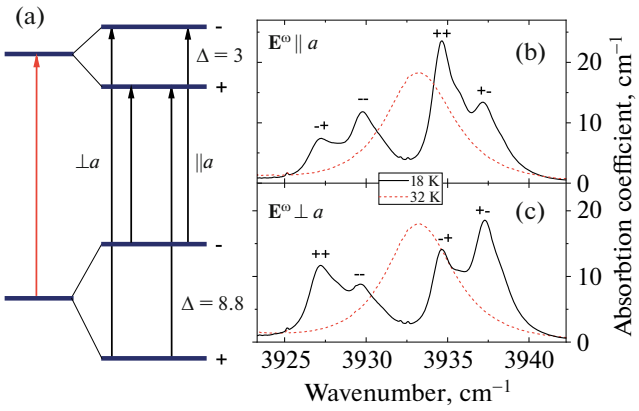

Fig. 5. (a) Diagrams of Kramers doublet splittings and optical transitions between splitting components and (b, c) the spectral line at 3933 cm^{-1} in the transition $^4I_{9/2} \rightarrow {}^4I_{13/2}$ at 33 K > T_N (dashed curve) and 18 K < T_N (continuous curves) for polarizations (b) $\mathbf{E}^\omega \parallel a$ (b) and (c) $\mathbf{E}^\omega \perp a$ (c).

ponents will be positive, whereas that of two others will be negative.

It should be noted that there are three equivalent directions C_2 in $NdFe_3(BO_3)_4$ crystal, so that three types of domain arise upon ordering. In each of the domains, the magnetic moments of iron are aligned along one of the C_2 axes. If the number of different domains is the same, the dichroism will be absent. The fact that the dichroism is observed experimentally indicates an excess amount of certain domains. The reason for this may be stress-induced anisotropy associated with magnetoelastic interactions [15].

In a two-level (in the paramagnetic phase) system, level splitting Δ grows linearly with internal exchange field B_{int}, $\Delta(T) \propto B_{int}(T)$, but the transition probabilities W_1 and W_2 remain unchanged. The increase in the degree of dichroism as the temperature drops below T_N can be explained as follows.

(i) Under the action of magnetic field the wavefunctions of different Stark levels mix up and change the transition probabilities quadratically depending on field (the exchange field grows with decreasing temperature) [16].

(ii) In $NdFe_3(BO_3)_4$ multiferroic, magnetic ordering induces spontaneous polarization [15]. It is natural to suppose the occurrence of local magnetostriction induced by an internal magnetic field resulting from magnetic ordering. Both effects quadratically depend on magnetic field [15], and both change the crystal field of a Nd^{3+} ion with the reduction of its symmetry. This, in turn, changes the transition probabilities and enhances the dichroism, which is, in the first approximation, linearly dependent on polarization and local strain because of striction, i.e., quadratically dependent on the field strength.

Figure 6 plots the experimental temperature dependence of the line splitting in the $NdFe_3(BO_3)_4$ spectrum, which shows the rise in internal field B_{int} in the position of Nd^{3+} ions, $\Delta(T) \propto B_{int}(T)$, and the dependence $\Delta^2(T) \propto B_{int}^2(T)$ versus the experimental dependence of linear dichroism LD(T). In the temperature range 30–17 K, the temperature variation of the dichroism is close to the dependence $\Delta^2(T) \propto B_{int}^2(T)$. A discrepancy may be associated with the ignorance of other mechanisms changing the probabilities of optical transitions during ordering of the magnetic moments of iron to form a collinear structure.

The gradual decrease in the dichroism when the temperature drops below 17 K correlates with the formation of a helicoidal structure of iron magnetic moments [2–4]. In a harmonic helicoidal phase, all directions in the basal plane are equivalent; the splitting values of Kramers doublets, which depend on the field strength alone, do not change (that is, the form of the spectrum remains the same); and the dichroism disappears. The fact that the dichroism persists even at very low temperatures may be related both to the anharmonicity of the helicoidal structure [3] and to the coexistence of the helicoidal and collinear magnetic phases, which was discovered in experiments on X-ray resonance magnetic scattering [4]. According to [4], as the temperature declines from T_{IC} down, the fraction of the helicoidal phase grows and that of the collinear phase drops roughly to 1/3 at 5 K. A rough estimate based on Fig. 6 gives for the dichroism at 5 K roughly 1/3 of its value expected in the absence of transition to the helicoidal structure. Thus, the low-temperature contribution of the helicoidal structure

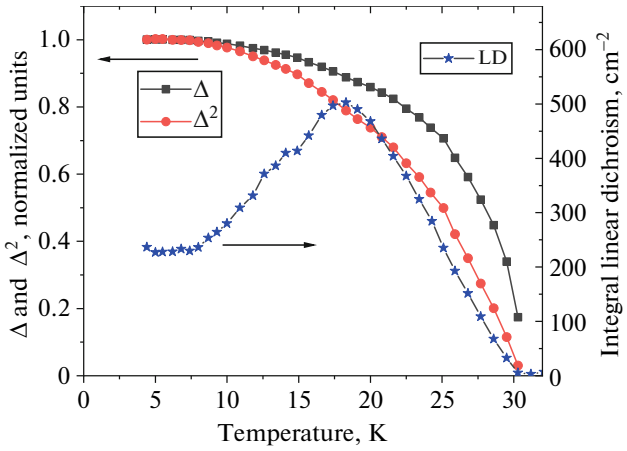

Fig. 6. Temperature dependences (for transition $^4I_{9/2} \rightarrow {}^4I_{3/2}$) $\Delta(T)$ (black squares) and $\Delta^2(T)$ (red circles) of spectral line splittings for $NdFe_3(BO_3)_4$ crystal and the temperature dependence of the integral lin1ear dichroism (blue asterisks).

anharmonicity to the residual dichroism is insignificant, if any.

It should be noted that the experimental temperature dependence of the dichroism (Fig. 4) can be explained otherwise, for example, by assuming that below 17 K the magnetic moments of iron start gently rotate, preserving collinearity, or that the number of domains with magnetic moments aligned along different C_2 axes becomes the same. To check whether such a scenario does take place, we performed relevant investigations at different temperatures of the complete polarization circle with a 5° step. Within an experimental error and irrespective of the temperature, the maximal dichroism in the spectra was observed when the polarizer was set along and normally to the same C_2 axis.

5. CONCLUSIONS

We studied linear optical dichroism in the basal plane of trigonal multiferroic crystal $NdFe_3(BO_3)_4$ in the range of *f–f* transitions in a Nd^{3+} ion. It was found that the dichroism arises at temperature $T_N \approx 30$ K of iron subsystem magnetic ordering into a collinear antiferromagnetic structure with magnetic moments aligned along one of the C_2 axes in the basal plane of the crystal. Accordingly, three types of domains are formed. The degree of dichroism was maximal when vector $\mathbf{E}^\omega$ of incident light was directed along or normal to one of the three C_2 axes. This indicates that domains of one type prevail possibly because of stress-induced anisotropy.

In the temperature interval 30–17 K, the dichroism grows and then, at further cooling down, gently decreases to about 1/3 of its maximal value. However, the field direction at which the dichroism is maximal does not change. Such behavior of optical linear dichroism is consistent with the smooth transition of the magnetic structure to an incommensurate helicoidal phase below 13.5–19 K [2–4, 9] and with the coexistence of the helicoidal and collinear phases at very low temperatures [4] but contradicts the concept of iron magnetic moments fluctuating within ±10° about the C_2 axis in the low-temperature phase [11].

In the first approximation, the growth of the linear dichroism in the temperature range where the order parameter of the antiferromagnetic collinear phase rises can be explained by the variation of the transition probabilities. The reasons for the probability variation may the following.

(i) The wavefunctions of different Stark levels mix up under the action of an internal magnetic field arising at Nd^{3+} ions in the course of iron subsystem magnetic ordering and (ii) spontaneous polarization and local striction induce changes of the crystal field.

FUNDING

This study was supported by the Ministry of Science and Higher Education (project no. FFUU-2022-0003) and partially (K.N. B., dichroism measurements) by the Russian Science Foundation (grant no. 19-72-10132P).

CONFLICT OF INTEREST

The authors declare that conflicts of interest are absent.

ADDITIONAL INFORMATION

This article is prepared for the memorial issue of the journal dedicated to the 95th birthday of L.A. Prozorova.

REFERENCES

1. A. K. Zvezdin, G. P. Vorob'ev, A. M. Kadomtseva, Yu. F. Popov, A. P. Pyatakov, L. N. Bezmaternykh, A. V. Kuvardin, and E. A. Popova, JETP Lett. **83**, 509 (2006).
2. P. Fisher, V. Pomjakushin, D. Sheptyakov, et al., J. Phys.: Condens. Matter **18**, 7975 (2006).
3. M. Janoschek, P. Fischer, J. Schefer, et al., Phys. Rev. B **81**, 094429 (2010).
4. J. E. Hamann-Borrero, S. Partzsch, S. Valencia, et al., Phys. Rev. Lett. **109**, 267202 (2012).
5. N. I. Leonyuk and L. I. Leonyuk, Prog. Cryst. Growth Charact. Mater. **31**, 179 (1995).
6. O. A. Alekseeva, E. S. Smirnova, K. V. Frolov, et al., Crystals **12**, 1203 (2022).
7. E. P. Chukalina, D. Y. Kuritsin, M. N. Popova, et al., Phys. Lett. A **322**, 239 (2004).
8. N. Tristan, R. Klingeler, C. Hess, et al., J. Magn. Magn. Mater. **316**, e621 (2007).
9. K. V. Frolov, I. S. Lyubutin, O. A. Alekseeva, et al., J. Alloys Compd. **909**, 164747 (2022).

10. L. E. Svistov, A. I. Smirnov, L. A. Prozorova, O. A. Petrenko, A. Ya. Shapiro, and L. N. Dem'yanets, JETP Lett. **80**, 204 (2004).
11. S. Nakamura, T. Masuda, K. Ohgushi, and T. Katsufuji, J. Phys. Soc. Jpn. **89**, 084703 (2020).
12. K. N. Boldyrev, R. V. Pisarev, L. N. Bezmaternykh, and M. N. Popova, Phys. Rev. Lett. **109**, 267202 (2012).
13. M. N. Popova, E. P. Chukalina, T. N. Stanislavchuk, et al., Phys. Rev.B **75**, 224435 (2007).
14. I. A. Gudim, E. V. Eremin, and V. L. Temerov, J. Cryst. Growth **312**, 2427 (2010).
15. A. M. Kadomtseva, Yu. F. Popov, G. P. Vorob'ev, A. P. Pyatakov, S. S. Krotov, and K. I. Kamilov, V. Yu. Ivanov, A. A. Mukhin, A. K. Zvezdin, A. M. Kuz'menko, L. N. Bezmaternykh, I. A. Gudim, and V. L. Temerov, J. Low Temp. Phys. **36**, 511 (2010).
16. M. N. Popova, T. N. Stanislavchuk, B. Z. Malkin, and L. N. Bezmaternykh, Phys. Rev. Lett. **102**, 187403 (2009).

Translated by V. Isaakyan